URSI - RCRS 2022, IIT (Indore), India, 1 - 4 December, 2022

Ground and Volume Scattering Separation in Compact Polarimentric Interferometric SAR Data

Subhadip Dey[(1)], Narayanarao Bhogapurapu[(2)], and Avik Bhattacharya[(2)]
(1) Microwaves and Radar Institute, German Aerospace Centre (DLR), Germany
(2) Microwave Remote Sensing Lab (MRSLab), Indian Institute of Technology Bombay, India

Abstract

This work presents a methodology to separate the ground and volume contributions from compact polarimetric SAR interferometric (PolInSAR) data over forest areas. One can decompose the PolInSAR data into two covariance matrices from ground and volume in a particular resolution cell, relying on the assumptions of the two-layer model. We demonstrate this approach using simulated single baseline compact polarimetric SAR data of the BioSAR-2008 mission over boreal forests in Northern Sweden.

1 Introduction

Polarimetric SAR Interferometry (PolInSAR) provides the advantage of getting the interferometric response of each pixel for various polarimetric combinations. Since the polarimetric response is sensitive to the scattering mechanisms, PolInSAR might help to get the detailed scattering characteristics within a resolution cell.

In this regard, coherent models based on two-layer assumptions have been used in forest and agriculture domains. Primarily, the assumption of a volume layer on top of the soil layer enables the estimation of different biophysical characteristics of the vegetation [1, 2]. Lopez-Sanchez et al. [3] estimated the vegetation height over winter rape and maize fields using airborne PolInSAR data. Later, Lavalle et al. [4] demonstrated the PolInSAR technique for compact polarimetric SAR data to characterize the forest canopy properties. This work demonstrates the separation of radar response of the ground and volume component within a resolution cell using compact polarimetric SAR data.

2 Methodology

Single baseline PolInSAR measurements consist of full polarimetric responses of the target from two different incidence angles. In this regard, the single baseline coherency matrix $\mathbf{T}_\mathrm{s}$ can be written as,

$$\mathbf{T}_\mathrm{s} = \langle \mathbf{k}\,\mathbf{k}^H \rangle = \begin{bmatrix} \mathbf{T}_{11} & \Omega_{12} \\ \Omega_{12}^H & \mathbf{T}_{22} \end{bmatrix} \tag{1}$$

where, $\mathbf{k}$ is the Pauli basis vectors for two acquisitions in a single baseline, $\mathbf{k} = \left[\mathbf{k}_1^T \mathbf{k}_2^T\right]^T$ and H indicates the complex conjugate. The Hermitian matrices, $\mathbf{T}_{11}$ and $\mathbf{T}_{22}$ denote the polarimetric contributions of the two acquisitions, whereas non-Hermitian Ω_{12} is the polarimetric as well as interferometric contribution. For compact polarimetric case, $\mathbf{T}_{11}, \mathbf{T}_{22}, \Omega_{12} \in \mathbb{C}^{2\times 2}$. Also, for compact polarimetric case (left circular transmit), $\mathbf{k}_i$ can be expressed as, $\mathbf{k}_{i\in(1,2)} = \frac{1}{\sqrt{2}}[S_{HH} + jS_{HV}, S_{HV} + jS_{VV}]$. Here, $S_{\mathrm{xy}}(\mathrm{x,\,y} \to H,V)$ are the elements of the scattering matrix of a full polarimetric acquisition. $\mathbf{T}_s$ is a complex Hermitian positive semi-definite 4×4 matrix.

According to the two-layer model assumptions, one can decompose the scattering phenomenon within a resolution cell into two physical constituents; the impermeable soil layer to the electromagnetic wave and a volume layer of vegetation canopy on the top of the soil layer. The concept of the two-layer model is also extended in interferometry, such as the Random Volume Over Ground (RVOG) model [2] and the Interferometric Water Cloud Model (IWM) [1]. Moreover, according to Cloude et al. [5], one can extend the scalar formation into a vector formation using a complex vector, $\mathbf{w}$, indicating different random scattering mechanisms. After projecting this complex vector, $\mathbf{w}$ onto the scattering vectors, $\mathbf{k}_{i\in(1,2)}$, the coherence between acquisitions i and j, $\gamma_{ij}(\mathbf{w})$ can be expressed as,

$$\gamma_{ij}(\mathbf{w}) = \frac{\mathbf{w}^H\,\Omega_{12}\,\mathbf{w}}{\sqrt{\mathbf{w}^H\,\mathbf{T}_{11}\,\mathbf{w}\cdot\mathbf{w}^H\,\mathbf{T}_{22}\,\mathbf{w}}} \tag{2}$$

2.1 Ground and volume coherency matrices separation

According to the two-layer model, one can separate the response of a resolution cell into the ground (soil) and volume components. Therefore, the polarimetric covariance matrices $(\mathbf{T}_{11}, \mathbf{T}_{22})$ as well as the the polarimetric-interferometry matrix (Ω_{12}) can be written as,

$$\mathbf{T}_{ii} = \mathbf{T}_g + \mathbf{T}_v \tag{3}$$

$$\Omega_{ij} = \gamma_{ij}^g \mathbf{T}_g + \gamma_{ij}^v \mathbf{T}_v \tag{4}$$

where $\mathbf{T}_g$ and $\mathbf{T}_v$ are the 2×2 Hermitian positive semi-definite ground and volume coherency matrices, respectively, and γ_{ij}^g and γ_{ij}^v are the ground and volume interferometric coherences, respectively. Now, if we replace the components of equation (3) and equation (4) in equa-

tion (2), we get,

$$\gamma_{ij}(\mathbf{w}) = \frac{\mathbf{w}^H \Omega_{12} \mathbf{w}}{\sqrt{\mathbf{w}^H \mathbf{T}_{11} \mathbf{w} \cdot \mathbf{w}^H \mathbf{T}_{22} \mathbf{w}}} = \frac{\gamma_{ij}^g \mu(\mathbf{w}) + \gamma_{ij}^v}{1 + \mu(\mathbf{w})} \quad (5)$$

These ground and volume coherences can be defined as,

$$\gamma_{ij}^{(p)} = \frac{\int F^p(z)\, e^{jk_{z(ij)}z}\, dz}{\int F^p(z)\, dz} \quad (6)$$

where, $k_{z(ij)}$ is the vertical wavenumber between acquisitions i and j, $F^p(z)$ indicates the vertical characteristics of the canopy and $p \in (g, v)$. Therefore, it can be seen from equation (5) that the coherence $\gamma_{ij}(\mathbf{w})$ is the linear segment defined by γ_{ij}^g and γ_{ij}^v with a control parameter, $\mu(\mathbf{w})$. This control parameter, $\mu(\mathbf{w})$, is known as the ground-to-volume ratio. $\mu(\mathbf{w})$ is defined as,

$$\mu(\mathbf{w}) = \frac{\mathbf{w}^H \mathbf{T}_g \mathbf{w}}{\mathbf{w}^H \mathbf{T}_v \mathbf{w}} \quad (7)$$

Further, the coherency matrix, $\mathbf{T}_\mathrm{s}$ can be decomposed as the sum of the Kronecker products [6] as,

$$\mathbf{T}_\mathrm{s} = \mathbf{R}_\mathrm{g} \otimes \mathbf{T}_\mathrm{g} + \mathbf{R}_\mathrm{v} \otimes \mathbf{T}_\mathrm{v} \quad (8)$$

where, $\mathbf{R}_\mathrm{g}$ and $\mathbf{R}_\mathrm{v}$ are the 2×2 structure matrices of the ground and volume, respectively. In order to reduce the polarimetric variability, a pre-whitening filter could be applied, which produces the interferometric coherences as the numerical range of the Π_{ij} matrices. Accordingly, the diagonal elements of the structure matrices, $\mathbf{R}_\mathrm{g}$ and $\mathbf{R}_\mathrm{v}$ reduce to unity, whereas the off-diagonal elements represent the coherences γ_{ij}^g and γ_{ij}^v. Therefore, one can write the matrix as,

$$\tilde{\mathbf{T}} = \mathbf{P}^{-\frac{1}{2}} \mathbf{T}_\mathrm{s} \mathbf{P}^{-\frac{1}{2}} = \begin{bmatrix} \mathbf{I} & \Pi_{12} \\ \Pi_{12}^H & \mathbf{I} \end{bmatrix} \quad (9)$$

where, $\mathbf{P} = \begin{bmatrix} \mathbf{T}_{11} & 0 \\ 0 & \mathbf{T}_{22} \end{bmatrix}$

Therefore, after pre-whitening equation (3) and equation (4) can be written as,

$$\mathbf{I} = \mathbf{T}_{gn} + \mathbf{T}_{vn} \quad (10)$$

$$\Pi_{ij} = \gamma_{ij}^g \mathbf{T}_{gn} + \gamma_{ij}^v \mathbf{T}_{vn} \quad (11)$$

where, $\mathbf{T}_{gn}$ and $\mathbf{T}_{vn}$ are the pre-whitened ground and volume coherency matrices, respectively and $\mathbf{I}$ is a 2×2 identity matrix. Therefore, when the ground and volume coherences are known, the matrices $\mathbf{T}_{gn}$ and $\mathbf{T}_{vn}$ can be written as,

$$\mathbf{T}_{vn} = H\left(\frac{\Pi_{ij} - \gamma_{ij}^g \mathbf{I}}{\gamma_{ij}^v - \gamma_{ij}^g}\right) \quad (12)$$

$$\mathbf{T}_{gn} = H\left(\frac{\Pi_{ij} - \gamma_{ij}^v \mathbf{I}}{\gamma_{ij}^g - \gamma_{ij}^v}\right) \quad (13)$$

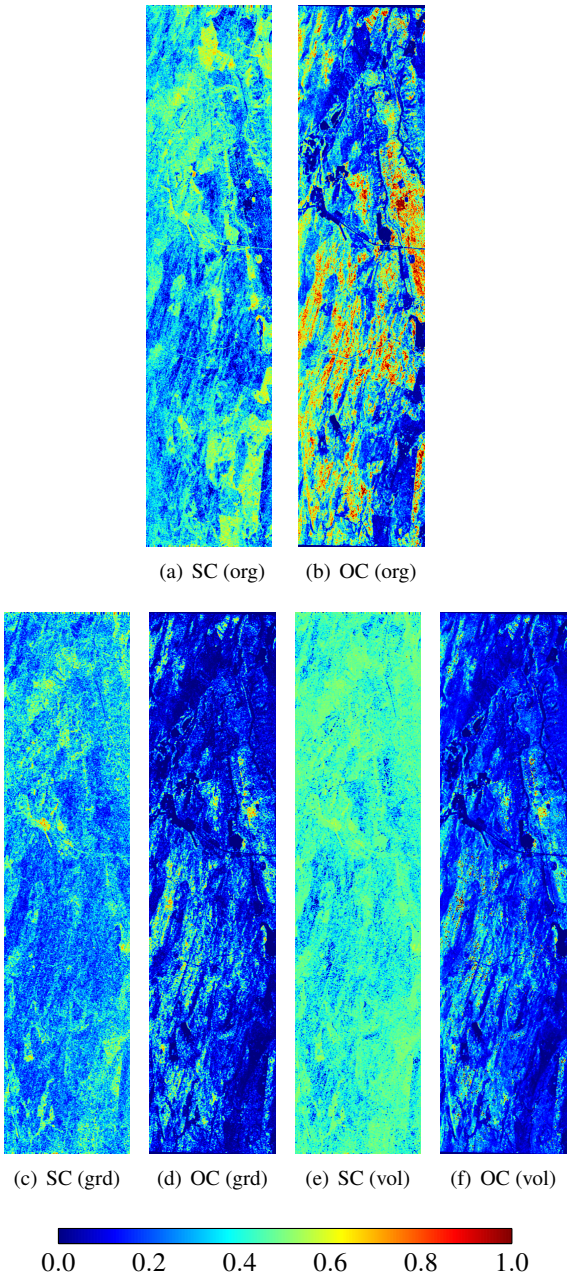

Figure 1. The Same Sense (SC) and Opposite Sense (OC) components for actual master image (org) and ground (grd) and volume (vol) responses using a slave image of spatial baseline of 16 m.

here, $H(\mathbf{A})$ denotes the Hermitian part of a matrix $\mathbf{A}$, $H(\mathbf{A}) = \frac{\mathbf{A} + \mathbf{A}^H}{2}$. For a single baseline case, the simple assumption is that the position of γ_{ij}^g is at the unit circle with the known phase. Therefore, one can draw the coherence line between γ_{ij}^g and the center of the mass of the coherence region, $\mathrm{tr}(\Pi)/2$. Further, the volume coherence can be estimated following the line until the end of the coherence region. This technique essentially ensures that both $\mathbf{T}_{gn}$ and $\mathbf{T}_{vn}$ are positive and semi-definite. However, one might note that all points outside the coherence region are valid as a volume coherence point. Hence, this estimate re-

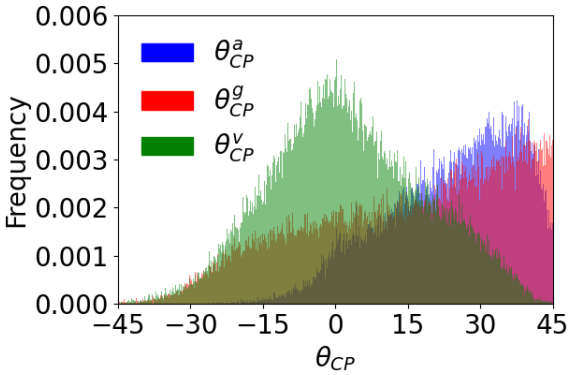

Figure 2. Histogram of the scattering type parameter for master image (θ^a_{CP}), ground response (θ^g_{CP}) and the volume response (θ^v_{CP}) for 16 m baseline slave image.

mains ambiguous. However, according to single baseline PolInSAR it is quite common to fix γ^v_{ij} at a point where, $\mu_{\min} = 0$. This assumption helps to get a ground coherency matrix of rank-2, i.e., a possible combination of a single-bounce and a double-bounce scattering mechanism.

The scattering-type parameter introduced by Dey et al. [7, 8] identifies diverse scattering characteristics from canonical and distributed targets with the help of 3D Barakat degree of polarization and the elements of the coherency matrix. In order to identify the changes of the scattering mechanisms from the original to the ground and volume coherency matrices, we have utilized the scattering type parameter, $\theta_{\mathrm{CP}} \in [-45°, 45°]$. For compact-pol SAR data θ_{CP} is defined as,

$$\tan\theta_{\mathrm{CP}(p)} = \frac{m_{\mathrm{CP}(p)}\, S_{0(p)}\, \left(\mathrm{OC}_{(p)} - \mathrm{SC}_{(p)}\right)}{\mathrm{OC}_{(p)}\, \mathrm{SC}_{(p)} + m^2_{\mathrm{CP}(p)}\, S^2_{0(p)}} \qquad (14)$$

where, $S_{0(p)}$ is the total power, $\mathrm{OC}_{(p)} = (S_0 + S_3)/2$ is the opposite sense component, $\mathrm{SC}_{(p)} = (S_0 - S_3)/2$ is the same sense component and S_3 is the fourth Stokes element representing the coherent circular scattering component.

3 Results and Discussion

We have assessed the ground and volume separation using the BioSAR2008 campaign data in this work. The BioSAR2008 campaign consists of L- and P-band fully polarimetric airborne ESAR data. In this work, we have utilized the P-band data of 14th October 2008. Five different spatial baselines dataset, approximately at −8 m, 8 m, 16 m, 24 m and 32 m are used to assess the polarimetric contributions for ground and volume components. The Same Sense (SC) and Opposite Sense (OC) images of the master data (org) and the separated ground (grd) and volume (vol) responses are shown in Fig. 1. We have also shown the histogram of the scattering type parameter in Fig. 2.

One can see from Fig. 1 that the SC component in the volume response is high due to the asymmetric scattering from

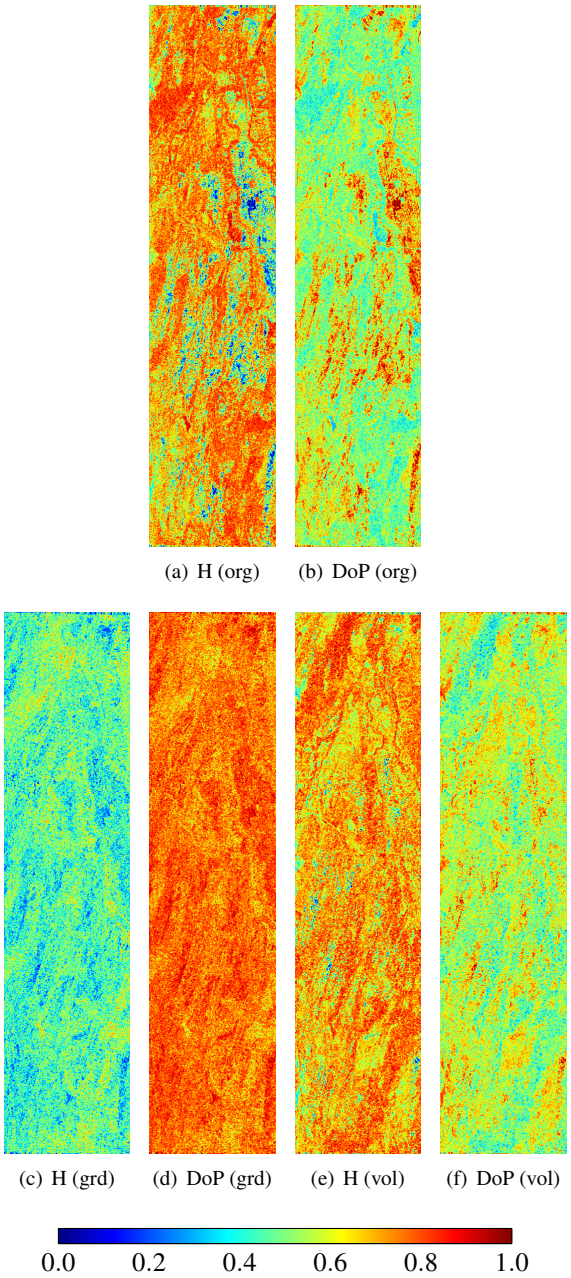

Figure 3. The entropy (H) and Degree of Polarization (DoP) components for actual master image (org) and for ground (grd) and volume (vol) responses using a slave image of spatial baseline of 16 m.

the canopy structure. Alternatively, the OC component is much higher in the ground response. However, the ground response affects the double bounce scattering in some cases due to the trunk and soil interface. Hence, we can observe high SC components in some areas.

The separation of ground and volume response can also be supported by the scattering type parameter (θ_{CP}) as shown in Fig. 2. One can see that the median of the histogram of the master image lies around 30°, indicating a mixture of volume components and symmetric with asymmetric scattering components. This separation of the volume compo-

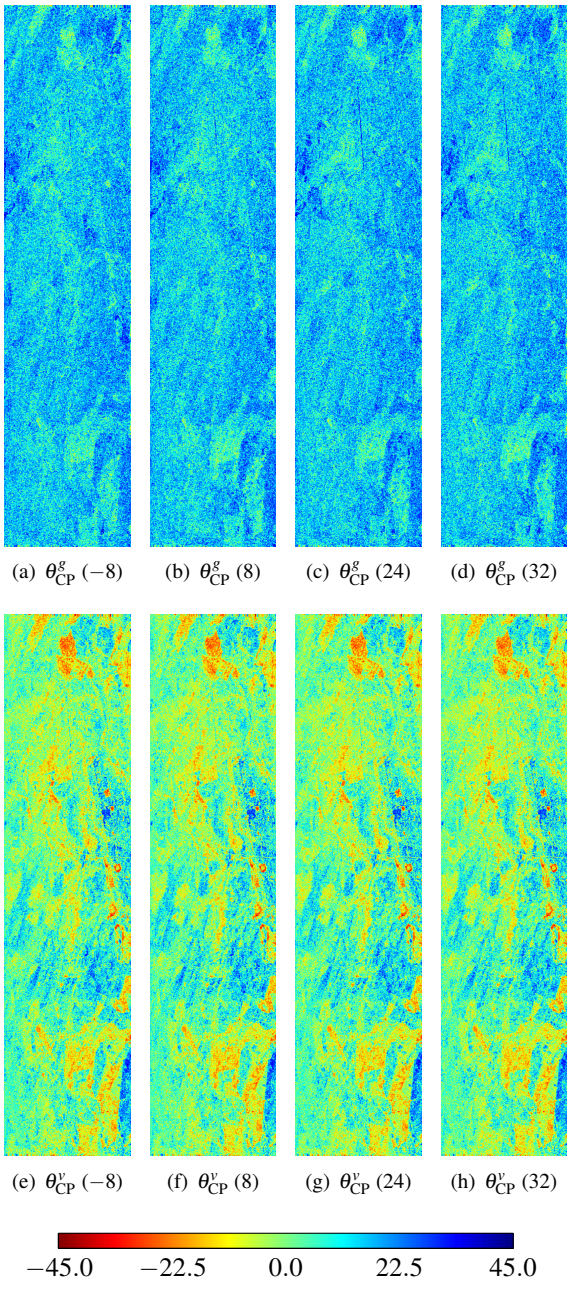

Figure 4. The variations of the scattering type parameter of ground (θ^g_{CP}) and volume (θ^v_{CP}) for spatial baselines of −8 m, 8 m, 24 m and 32 m.

nent from the symmetric-asymmetric components can be adequately seen from the histogram of ground (θ^g_{CP}) and volume (θ^v_{CP}) components. The median of θ^v_{CP} is around 0°, indicating the response from the volume component as either diffused or an equal mixture of regular and irregular scattering. In contrast, the median of θ^g_{CP} around 42° indicates the major scattering component towards the single bounce scattering. However, we can observe a stretch of θ^g_{CP} from $\approx -30°$ which is due to the double bounce scattering from the trunk-soil interface, as mentioned earlier.

We have also shown the entropy (H) and Degree of Polarization (DoP) plots in Fig. 3. One can see that the values of H in the ground component are lower than those of H in the volume component due to the assumption of a random volume of vegetation on the top of the soil in the model. Moreover, the DoP values in the ground component are higher than the volume component. These higher values essentially indicate the canonical scattering mechanisms from the ground. The images of θ^g_{CP} and θ^v_{CP} over other baselines are shown in Fig. 4.

4 Conclusion

This work demonstrates an approach to separate the ground and volume contribution from a single baseline PolInSAR measurement. A common procedure to fix the volume coherence at the end of the coherence region is followed to get the uniqueness in the volume component and generate a rank-2 ground component. The obtained ground and volume components provide better separation capability in terms of the scattering type parameter (θ_{CP}) and the scattering entropy (H) as well as the Degree of Polarization (DoP).

5 Acknowledgement

The authors would like to thank European Space Agency (ESA) for providing the BioSAR2008 campaign data.

References

[1] J. I. Askne, P. B. Dammert, L. M. Ulander, and G. Smith, "C-band repeat-pass interferometric SAR observations of the forest," *IEEE Trans. Geosci. Remote Sens.*, vol. 35, no. 1, pp. 25–35, 1997.

[2] S. Cloude and K. Papathanassiou, "Three-stage inversion process for polarimetric SAR interferometry," *IEE Proceedings-Radar, Sonar and Navigation*, vol. 150, no. 3, pp. 125–134, 2003.

[3] J. M. Lopez-Sanchez, I. Hajnsek, and J. D. Ballester-Berman, "First demonstration of agriculture height retrieval with PolInSAR airborne data," *IEEE Geosci. Remote Sens. Lett.*, vol. 9, no. 2, pp. 242–246, 2011.

[4] M. Lavalle, D. Solimini, E. Pottier, and Y.-L. Desnos, "Compact polarimetric SAR interferometry," *IET radar, sonar & navigation*, vol. 4, no. 3, pp. 449–456, 2010.

[5] S. R. Cloude and K. P. Papathanassiou, "Polarimetric SAR interferometry," *IEEE Trans. Geosci. Remote Sens.*, vol. 36, no. 5, pp. 1551–1565, 1998.

[6] S. Tebaldini, "Algebraic synthesis of forest scenarios from multibaseline PolInSAR data," *IEEE Trans. Geosci. Remote Sens.*, vol. 47, no. 12, pp. 4132–4142, 2009.

[7] S. Dey, A. Bhattacharya, D. Ratha, D. Mandal, and A. C. Frery, "Target characterization and scattering power decomposition for full and compact polarimetric SAR data," *IEEE Trans. Geosci. Remote Sens.*, vol. 59, no. 5, pp. 3981–3998, 2020.

[8] S. Dey, A. Bhattacharya, A. C. Frery, C. López-Martínez, and Y. S. Rao, "A model-free four component scattering power decomposition for polarimetric SAR data," *IEEE J. Sel. Top. Appl. Earth Obs. Remote Sens.*, vol. 14, pp. 3887–3902, 2021.